APPLIED AND ENVIRONMENTAL MICROBIOLOGY, Oct. 2002, p. 4827–4834 Vol. 68, No. 10
0099-2240/02/$04.00+0 DOI: 10.1128/AEM.68.10.4827–4834.2002

Characterization and Implications of the Cell Surface Reactivity of *Calothrix* sp. Strain KC97

V. R. Phoenix,[1] R. E. Martinez,[1] K. O. Konhauser,[2] and F. G. Ferris[1]*

Department of Geology, University of Toronto, Toronto, Ontario M5S 3B1, Canada,[1] and School of Earth Sciences, University of Leeds, Leeds LS2 9JT, United Kingdom[2]

Received 25 March 2002/Accepted 11 July 2002

The cell surface reactivity of the cyanobacterium *Calothrix* sp. strain KC97, an isolate from the Krisuvik hot spring, Iceland, was investigated in terms of its proton binding behavior and charge characteristics by using acid-base titrations, electrophoretic mobility analysis, and transmission electron microscopy. Analysis of titration data with the linear programming optimization method showed that intact filaments were dominated by surface proton binding sites inferred to be carboxyl groups (acid dissociation constants [pK_a] between 5.0 and 6.2) and amine groups (mean pK_a of 8.9). Sheath material isolated by using lysozyme and sodium dodecyl sulfate generated pK_a spectra similarly dominated by carboxyls (pK_a of 4.6 to 6.1) and amines (pK_a of 8.1 to 9.2). In both intact filaments and isolated sheath material, the lower ligand concentrations at mid-pK_a values were ascribed to phosphoryl groups. Whole filaments and isolated sheath material displayed total reactive-site densities of 80.3×10^{-5} and 12.3×10^{-5} mol/g (dry mass) of cyanobacteria, respectively, implying that much of the surface reactivity of this microorganism is located on the cell wall and not the sheath. This is corroborated by electrophoretic mobility measurements that showed that the sheath has a net neutral charge at mid-pHs. In contrast, unsheathed cells exhibited a stronger negative-charge characteristic. Additionally, transmission electron microscopy analysis of ultrathin sections stained with heavy metals further demonstrated that most of the reactive binding sites are located upon the cell wall. Thus, the cell surface reactivity of *Calothrix* sp. strain KC97 can be described as a dual layer composed of a highly reactive cell wall enclosed within a poorly reactive sheath.

The bacterial surface acts as a highly reactive interface due to an abundance of reactive constituents, such as carboxyl, hydroxyl, phosphoryl, and amine groups. These surface functional groups deprotonate with increasing pH and thus impart to the microorganism a net negative surface charge (1, 5, 11). Recently, the proton binding and charge properties of bacterial surfaces have been investigated in detail by using acid-base titrations to determine the types and abundances of these ligands (5, 6, 11, 26, 41). A prime reason for such investigations is to determine the capacity of bacteria to sorb cations from the aqueous environment. Such quantitative approaches are required for accurate modeling of the mechanisms by which microbes may inhibit metal transport in an aqueous system, with a view toward the use of bacteria as biofilters for toxic-metal remediation.

Other studies have investigated how surface chemistry and charge characteristics may influence such aspects as a microorganism's hydrophobicity (45, 48), its resistance to predation by phagotrophs (27, 48), its ability to adhere to a solid surface (19, 38, 45), and its resistance to toxins (15). Evidently, variations in such surface characteristics of bacteria have the potential to influence a wide variety of important ecophysiological factors.

The use of acid-base titration methods to determine cell surface functional-group reactivity has provided great insight into a wide variety of gram-positive and gram-negative bacteria (e.g., 5, 6, 11, 41), yet to our knowledge such a detailed study has still to be performed on cyanobacteria. This type of study is of particular interest as, on both a structural and a molecular level, cyanobacteria are complex prokaryotes. For example, although the cyanobacterial cell wall is gram negative in structure, the peptidoglycan layer tends to be much thicker, as in gram-positive bacteria, and exhibits a higher degree of cross-linkage between the peptidoglycan chains (for reviews, see references 7 and 18). Furthermore, although cyanobacterial cell walls lack teichoic acid, specific polysaccharides are covalently bound to the peptidoglycan in a manner not dissimilar to that seen in gram-positive bacteria (21, 23). Additionally, components commonly found in the cyanobacterial outer membrane, such as atypical fatty acids and carotenoids, are rarely present in other gram-negative bacteria (22, 33, 37).

Many recent studies of bacterial surfaces using the acid-base titration approach have focused on the cell wall (5, 6, 11, 41), but for a number of bacteria (including cyanobacteria), the cell wall is not the outermost surface of the microorganism because the microorganism produces an extracellular network of polysaccharides and proteins, such as capsules, slime, and more-structured sheaths. The functions of cyanobacterial exopolymers are many. A coating of extracellular polysaccharides may protect against dehydration (8, 17, 38) or provide chemically reactive sites capable of protecting the cell proper against detrimental metal uptake or biomineralization (31, 38, 46). Exopolymers may also protect against predation (8, 48) or aid in adhesion to a solid substrate (8, 38). As it is possible that surface charge density may influence some of these characteristics, an understanding of the exopolymer's electrochemistry is pertinent.

* Corresponding author. Mailing address: Department of Geology, 22 Russell St., University of Toronto, Toronto, Ontario M5S 3B1, Canada. Phone: (416) 978-0526. Fax: (416) 978-3938. E-mail: ferris@geology.utoronto.ca.

In this study, acid-base titrations were performed on whole filaments and separated exopolymeric sheath material of the filamentous cyanobacterium *Calothrix* sp. strain KC97, an isolate from the Krisuvik hot spring, Iceland. Data from titrations were analyzed by using a linear programming regression method (LPM) (for examples, see references 3, 5, and 40) to determine acid dissociation constants (pK_a) and site densities for proton binding sites on the cell surface. Electrophoretic mobility (EPM) and transmission electron microscopy (TEM) analyses were also used to assess the surface charge characteristics of *Calothrix* sp. strain KC97.

MATERIALS AND METHODS

Microorganism and cultivation. The filamentous cyanobacterium *Calothrix* sp. strain KC97, an isolate from the Krisuvik hot spring, Iceland (see reference 31 for details of isolation), was from the culture collection of V. R. Phoenix, Department of Geology, University of Toronto. The cyanobacteria were cultured in static Erlenmeyer flasks containing 100 ml of BG11 −N liquid medium (34) at 30°C and illuminated with cool white fluorescent light (700 lx). The cultures used in these experiments were 4 to 5 weeks old; i.e., they were mature, healthy cultures that lacked any notable presence of hormogonia. Hormogonia were required to be absent as filaments in this transient phase lack extracellular polysaccharides and are thus likely to have very different surface chemistries than those of mature, vegetative filaments.

Sheath separation. The method of sheath separation was based upon that described by Weckesser et al. (46) and is summarized as follows. Cultures of *Calothrix* sp. strain KC97 were washed three times by centrifugation at 3,000 × *g* in 18-MΩ ultrapure water. The washed culture was then suspended in 20 mM Tris-HCl buffer, pH 8. This material was homogenized by passage twice through a French pressure cell at 83 MPa (prior to each pass, the material was ultrasonicated for 5 min). The homogenate was then centrifuged at 20,000 × *g* for 10 min, and the supernatant was decanted. The pellet was resuspended in 200 mg of lysozyme (chicken egg white; EC 3.2.1.17) per liter in 20 mM ammonium acetate (pH 6.8), sonicated briefly to disperse the pellet, and then incubated for 16 h at 37°C with gentle mixing on an oscillator at 150 rpm. After incubation, the material was centrifuged at 20,000 × *g* for 30 min, and the supernatant was decanted. The remaining pellet was resuspended in 100 ml of 18-MΩ water, briefly sonicated, and then added drop-wise to 100 ml of boiling 4% (wt/vol) sodium dodecyl sulfate (final concentration, 2% [wt/vol]). After boiling for 15 min, the sheath material was then washed seven times in 18-MΩ water by centrifugation at 20,000 × *g*. For acid-base titrations and EPM analysis, the washed sheath material was resuspended in 0.01 M KNO_3 (pH ~5.5) and briefly ultrasonicated to disperse the pellet. Both acid-base titrations and EPM analysis of isolated sheath material were performed directly after the sheath material was isolated.

Acid-base titrations. Acid-base titrations were performed on both intact cyanobacteria and isolated sheath material to assess pK_a and site densities of proton binding sites. First, a 15-ml aliquot of the cyanobacterial culture was transferred to an acid-washed 250-ml polypropylene bottle and centrifuged at 20°C for 8 min at 10,400 × *g*. The growth medium was then discarded, and the filaments were washed a further four times in 100 ml of 18-MΩ water, again by centrifugation (10,400 × *g*, 8 min). The washed filaments were then suspended in 50 ml of 0.01 M KNO_3 (pH ~5.5).

Approximately 10 to 20 ml of the cyanobacterial suspension was then transferred to a 100-ml titration flask containing 200 μl of 0.2 M HNO_3, and 0.01 M KNO_3 was added to reach a final volume of 50 ml. This acidified cyanobacterial suspension was then covered with an airtight lid fitted with an N_2 gas line interface (the system was purged continually with N_2 during the experiment to prevent carbonate formation from CO_2 dissolution) and a precalibrated pH electrode connected to an autotitrator (Metrohm Titrino GP 736). During the experiment, the solution was stirred with an acid-washed magnetic stirring bar. Before titration, the system was allowed to equilibrate until the fluctuation in the pH reading was less than 0.5 mV/min for a period of at least 25 min. Aliquots of carbonate-free 0.01 M NaOH (see reference 5 for a description of base preparation) were delivered from the autotitrator's burette into the cyanobacterial suspension to increase the pH by increments of approximately 0.1 unit. The titration was run from pH 3 (the starting pH of the cyanobacterial suspension) through pH 12. Blank control titrations (i.e., without cyanobacteria) were also performed. The dry mass of titrated cyanobacteria was determined at the end of titration by filtration through 0.2-μm-pore-size Supor filters and air drying at 70°C to a constant weight. Acid-base titrations were similarly performed upon isolated sheath material, again from pHs 3 to 12. The details of sheath isolation and preparation are described above.

Determination of pK_a and site densities from titration data. The deprotonation of a monoprotic (containing one proton) functional group on the cyanobacterial surface can be described as follows:

$$HL \leftrightarrow L^- + H^+ \quad (1)$$

where L^- corresponds to a proton binding site on the cell surface and H^+ represents the proton in solution. The apparent equilibrium constant (K_a) for the reaction in equation 1 can be defined as

$$K_a = \frac{[H^+] \cdot [L^-]}{[HL]} \quad (2)$$

Discrete pK_a spectra, where pK_a equals $-\log K_a$, were generated from the titration data by using LPM. This computational approach has been used previously (5, 41) to determine site densities and pK_a for proton binding sites on bacterial surfaces.

In this study we focused on data collected over the pH range of 4 to 9, as errors for acid-base titrations increase outside this range (40). Viability checks using phycoerythrin autofluorescence (this phycobilin is dispersed rapidly upon lysis) and performed with a Nikon Microphot-FXA fluorescence microscope revealed that cell viability was >95% both before titration and throughout the titration range of interest.

Electrophoretic mobility. EPM measurements were performed to assess the net surface charge characteristics of isolated sheath material and whole filaments. Sheath material was isolated, washed, sonicated, and suspended in 0.01 M KNO_3 as described above. Intact *Calothrix* filaments were broken in a glass tissue grinder with a Teflon pestle to fragment the filaments into particles suitable for analysis. These were then washed three times in 18-MΩ water by centrifugation at 3,000 × *g* and suspended in 0.01 M KNO_3. Both isolated sheath material and fragmented filament suspensions had pHs of 5.5. EPM analyses were then performed with a Laval Lab Zetaphoremeter III at 23°C, in an electric field of 8.34 V/cm. After completion of EPM analysis at pH 5.5, the pH of the sheath suspension was increased to 12.2 with 0.1 M NaOH and EPM analysis was again performed.

TEM. Samples of *Calothrix* were fixed in 2% glutaraldehyde and processed for TEM as described previously (31). To qualitatively visualize the electronegativity of the cyanobacterial cross section, ultrathin sections were stained with a uranyl acetate solution (15% [wt/vol] uranyl acetate in methanol) for 10 min and with a lead citrate solution [2.66% (wt/vol) $Pb(NO_3)_2$ plus 3.52% (wt/vol) sodium citrate in 0.16 M NaOH] for 5 min. TEM was performed as described previously (31).

RESULTS

Titration of isolated sheath material. Treatment with lysozyme and sodium dodecyl sulfate successfully separated the sheath material from the trichomes as illustrated in Fig. 1, which shows the isolated material composed of clear, colorless empty sheath fragments. The pK_a spectra and site densities of surface proton binding sites from six replicate acid-base titrations of isolated sheath material are shown in Fig. 2. Note that the site densities are normalized to the mass of whole filaments from which the sheath material was isolated (as opposed to the dry mass of the sheath material alone) to allow comparison with data for whole, intact filaments. Inspection of the data shown in Fig. 2 reveals that the pK_a cluster into five distinguishable ligand classes (labeled A to E). Each class is suggested to represent the deprotonation of a certain type of functional group (e.g., carboxyl, phosphoryl, or amine) on the bacterial surface (Table 1). The attribution of functional groups to each ligand class is described in detail later, in Discussion.

The numerical details of each ligand class are recorded in Table 1. For each ligand class, a weighted mean pK_a, which was weighted by the site density of each component peak, was

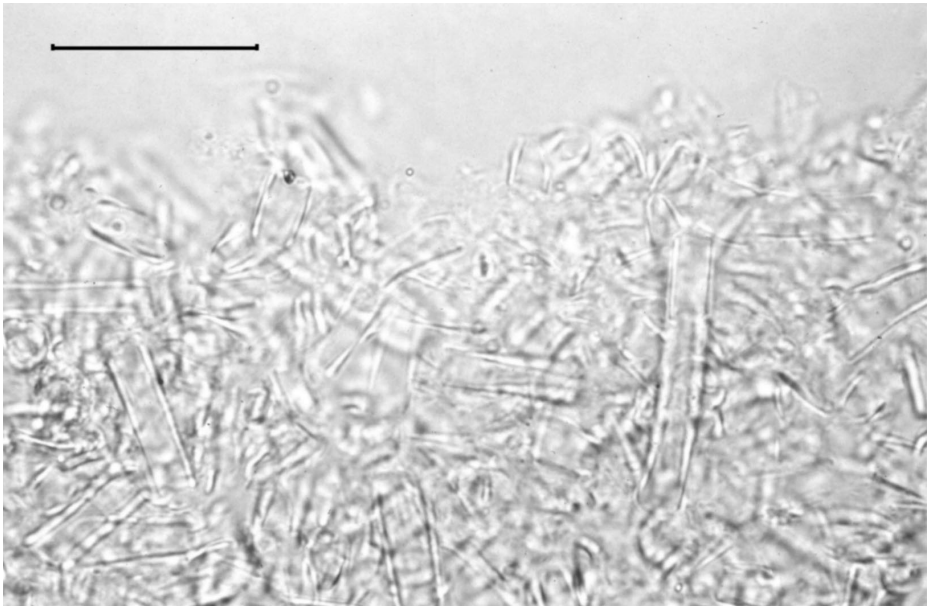

FIG. 1. Light micrograph of sheaths isolated from *Calothrix* sp. strain KC97 cells. The classic sheath morphology of colorless and empty tubes is clearly visible. Scale bar, 50 μm.

determined (Table 1). Additionally, the standard deviations for the spread of pK_a within each ligand class are shown in parentheses. The mean ligand concentrations (site densities) along with corresponding standard deviations are also given in Table 1.

Analysis of the sheath titration data revealed an average total proton binding site density (i.e., the sum of all reactive sites detected across the analyzed pH range) of 82.3×10^{-5} mol/g (dry mass) of sheath. Furthermore, mass balance measurements during isolation established that the sheath material contributes 15% of the dry mass of whole filaments and, thus, the sheath contributes only 12.3×10^{-5} mol/g to the total site density of the whole, intact microorganism.

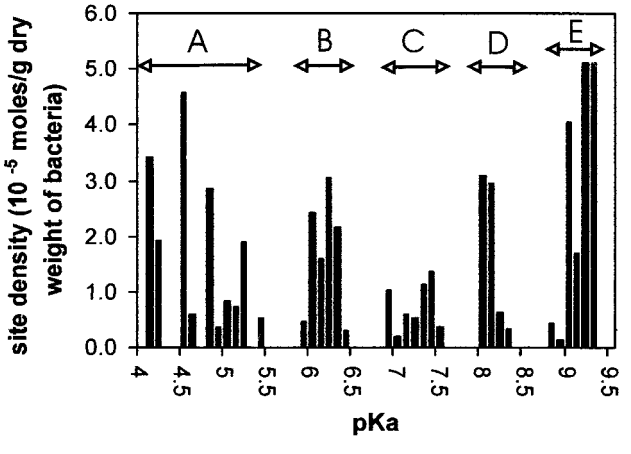

FIG. 2. pK_a spectrum for isolated sheaths, titrated in 0.01 M KNO_3 (composite plot of six filtrations). The concentration (site density) at each pK_a is normalized to the dry mass of cyanobacteria from which the sheath was isolated. The pK_a are suggested to cluster into five separate groups, which are labeled A to E.

Titration of intact filaments. During titration of the intact viable filaments, both the permeable sheaths and the enclosed cell walls are able to exchange protons with the surrounding media and thus both components of the cell envelope contribute to the generated pK_a spectrum shown in Fig. 3 and Table 2. Here, the generated pK_a spectrum is suggested to cluster into six distinguishable ligand classes, labeled U to Z (Fig. 3 and Table 2). Again, the attribution of functional groups to each ligand class is described in detail later, in Discussion.

Summation of the ligand concentrations across the analyzed pH range reveals that whole filaments of *Calothrix* sp. strain KC97 exhibit an average total site density of 80.3×10^{-5} mol/g of cyanobacteria. Interestingly, as stated above, the sheath material contributes only 12.3×10^{-5} mol/g of cyanobacteria to this total, implying that much of the surface reactivity of whole filaments is located on the cell walls and not on the sheaths. This is highlighted by comparing the pK_a spectra for isolated sheaths (Fig. 2) with the spectra for whole filaments

TABLE 1. Composite titration data for isolated sheaths[a]

Ligand class (pK_a cluster in Fig. 2)	No. of occurrences[b]	Mean pK_a (SD)[d]	Mean L_T (10^{-5} mol/g of bacteria)[c,d]	Suggested functional group
A	6	4.62 (0.39)	3.3 (1.8)	Carboxyl
B	6	6.12 (0.14)	2.7 (0.6)	Carboxyl or phosphoryl
C	5	7.26 (0.22)	1.4 (0.3)	Phosphoryl
D	5	8.07 (0.11)	2.3 (0.9)	Amine
E	5	9.15 (0.18)	4.1 (2.1)	Amine

[a] Mean site densities (L_T), pK_a, and suggested functional groups are shown for ligand classes A to E identified in Fig. 2.

[b] Number of occurrences is the number of titrations which show a pK_a peak within the ligand range (maximum, 6).

[c] Site densities (L_T) are normalized to the dry mass of cyanobacteria from which the sheath was isolated.

[d] Values in parentheses are standard deviations ($\sigma = 1$).

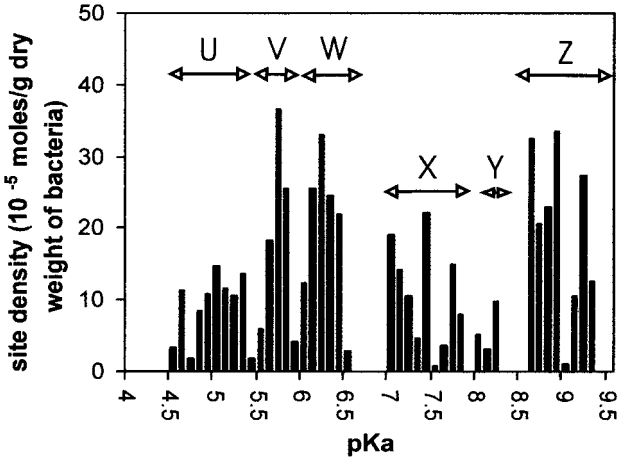

FIG. 3. pK_a spectrum for intact filaments of *Calothrix* sp. strain KC97, titrated in 0.01 M KNO_3 (composite plot of 11 filtrations). The concentration (site density) at each pK_a is normalized to the dry mass of cyanobacteria used. The pK_a are suggested to cluster into six groups, which are labeled U to Z.

(Fig. 3). Clearly, a higher density of binding sites is displayed by the surfaces of whole filaments than by the sheaths alone.

EPM. EPM measurements of isolated sheath fragments show that the sheath exhibits a net surface charge that is close to neutral (average, +0.1 μm/s/V/cm) at pH 5.5 (Fig. 4a). Increasing the pH caused a slight increase in the negative charge of the sheath (average, −0.65 μm/s/V/cm at pH 12.2) (Fig. 4a).

EPM analysis of fragmented whole filaments of *Calothrix* consistently produced dual peaks at pH 5.5, one around −2.5 μm/s/V/cm and a broader peak at 0 to −1 μm/s/V/cm (Fig. 4b).

TEM. As shown in Fig. 5, the cell wall is electron opaque and thus has bound significant quantities of the heavy metal stain, indicating the presence of abundant negatively charged reactive binding sites. In comparison, the sheath is relatively electron translucent due to weaker binding of the heavy metals and thus contains a much lower density of reactive sites. This is consistent with the titration data, which show that the cell wall contains a greater density of proton binding sites than the sheath.

TABLE 2. Composite titration data for intact *Calothrix* filaments[a]

Ligand class (pK_a cluster in Fig. 3)	No. of occurrences[b]	Mean pK_a (SD)[c]	Mean L_T (10^{-5} mol/g bacteria)[c]	Suggested functional group
U	10	5.02 (0.25)	18.9 (6.2)	Carboxyl
V	5	5.70 (0.13)	20.4 (22.0)	Carboxyl
W	9	6.23 (0.16)	25.0 (13.0)	Phosphoryl or carboxyl
X	11	7.34 (0.25)	15.5 (4.6)	Phosphoryl
Y	3	8.13 (0.08)	7.3 (5.0)	Phosphoryl or amine
Z	11	8.92 (0.23)	19.9 (10.4)	Amine

[a] Mean site densities (L_T), pK_a, and suggested functional groups are shown for ligand classes U to Z identified in Fig. 3.
[b] Number of occurrences is the number of titrations which show a pK_a peak within the ligand range (maximum, 11).
[c] Values in parentheses are standard deviations ($\sigma = 1$).

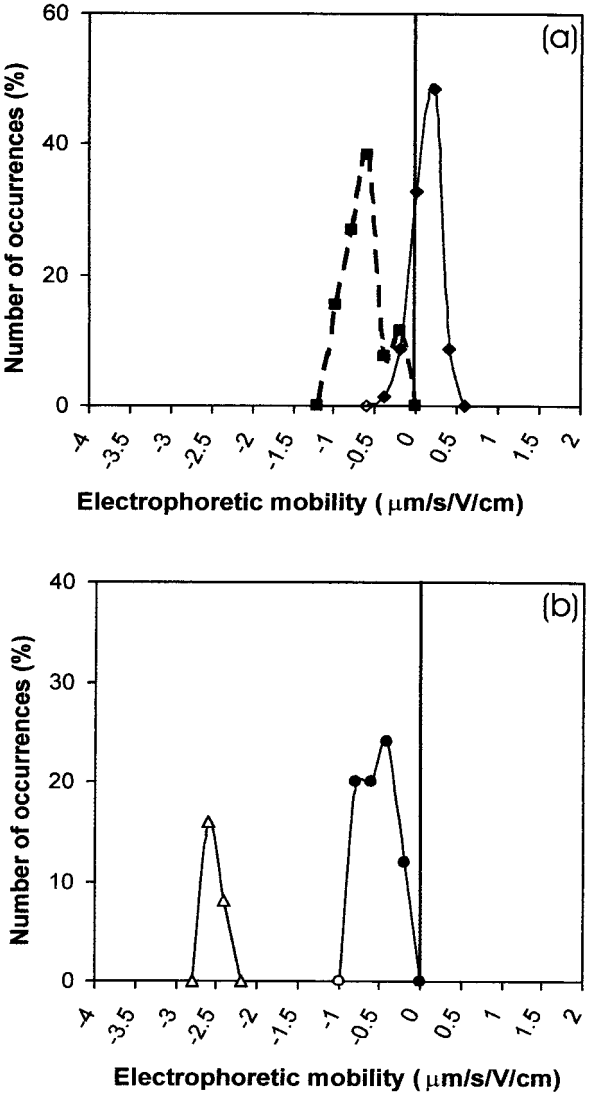

FIG. 4. EPM measurements performed in 0.01 M KNO_3. (a) Results for isolated sheath material: (—), EPM at pH 5.5; (----), EPM at pH 12.2. (b) Results for fragmented whole filaments at pH 5.5. Note the typical dual peaks recorded for this material. The right-hand peak is suggested to represent predominantly ensheathed filaments and the left peak is suggested to represent unsheathed cells.

DISCUSSION

Interpretation of pK_a spectra. Previous biochemical studies of the sheaths of similar *Calothrix* species, which utilized the same sheath isolation procedure, revealed that this exopolymer is composed predominantly of neutral sugars, along with smaller quantities of galacturonic and amino acids (46). By combining this knowledge of sheath composition with knowledge of pK_a values of known model compounds, it is possible to infer which organic functional groups within the sheath are likely to be responsible for each ligand class in the pK_a spectrum for isolated sheath material (Fig. 2 and Table 1). It should be stated here that electronic and steric interactions in complex biological molecules may result in pK_a which differ slightly from those of model compounds (43). These effects are diffi-

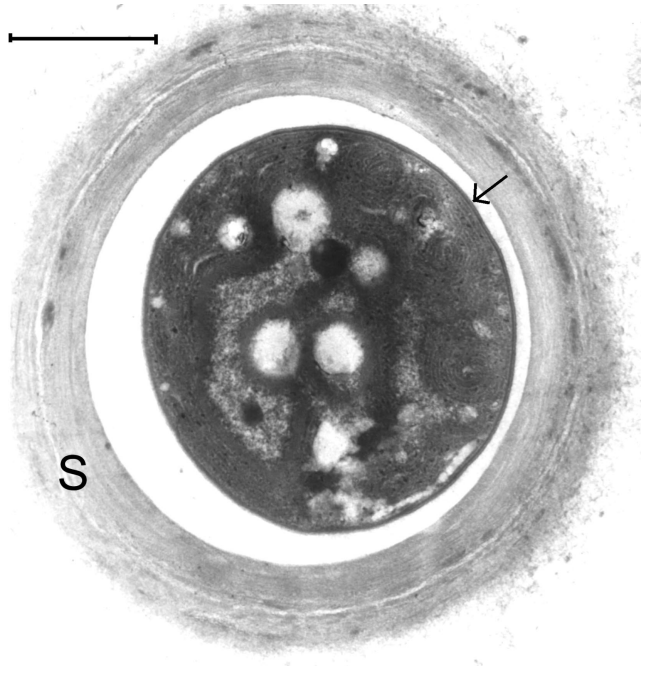

FIG. 5. TEM of a cross section through a filament of *Calothrix* sp. strain KC97, stained with uranyl acetate and lead citrate. Note that the cytoplasm and, in particular, the cell wall (indicated by an arrow) are electron opaque and thus contain a high density of electronegative sites. In contrast, the sheath (S) is stained more lightly and thus contains fewer electronegative sites. Scale bar, approximately 2 μm.

cult to quantify accurately (5), and thus the functional groups assigned to pK_a clusters are simply those that are most consistent with available compositional information (46).

Carboxylic functional groups deprotonate over a low pH range and predominantly exhibit pK_a between 2 and 6 (30). Thus, ligand class A, and possibly B (Fig. 2, Table 1), is likely to be representative of carboxyl groups contained within the galacturonic acid of the sheath. Similarly, data from model compounds reveal that phosphoryl groups commonly exhibit intermediate pK_a between 5.4 and 8 (25). Thus, ligand classes C and B (Fig. 2 and Table 1) can be attributed to the deprotonation of phosphoryl groups. Interestingly, the levels of phosphate recorded in the sheaths of *Calothrix* spp. are low (46), and in consideration of this it is suggested that ligand class B may be better ascribed to the more common carboxyl groups. Certainly, ligand class B exhibits a mean pK_a of 6.12 (Table 1), which is well within the known range of expected pK_a for carboxyl groups which predominate between ~2 and 6, but it can exhibit pK_a as low as 2 or as high as 8 (30).

Amine groups commonly exhibit pK_a between 8 and 11 (25). Ligand classes D and E, which exhibit mean pK_a of 8.07 ± 0.11 and 9.15 ± 0.18, respectively, are therefore suggested to be representative of deprotonation of amino acids contained within the sheath. Hydroxyl groups, such as those abundant on the neutral sugars, do not usually deprotonate until the pH is ~12 (30) and thus would not be detected with the present LPM and experimental conditions.

The same approach can be used to infer which organic functional groups within the cell envelope are likely to be responsible for each ligand class in the pK_a spectrum for whole filaments (Fig. 3 and Table 2). As mentioned previously, both the cell wall and the sheath contribute to the generated pK_a spectrum. Based upon the range of pK_a for known compounds described above, ligand classes U and V (Fig. 3 and Table 2) are attributed to carboxyl groups found in abundance in cell wall constituents such as diaminopimelic and glutamic acids in the peptide cross-linkages of peptidoglycan (20, 23). Additional carboxyl groups may be provided by fatty acids such as β-hydroxypalmitic acid (36, 47), a component of the lipid A fraction rarely detected in the lipopolysaccharide (LPS) of most gram-negative bacteria but common in most cyanobacteria (7). Carboxyl groups are also found in the sheath, as described above. Carboxylated teichoic acids, covalently bound to peptidoglycan, do not occur within the cell walls of cyanobacteria. However, in cyanobacteria such as *Synechocystis* sp. strain PCC 6714, the peptidoglycan forms a complex with polysaccharides which are bound to the muramic acid 6-phosphate component of the peptidoglycan via phosphodiester bonds (23). Thus, if these phosphate-bound polysaccharides are similarly found in *Calothrix* sp. strain KC97, then they likely contribute to ligand classes W and X (Fig. 3 and Table 2). Other phosphoryl-containing polymers in the cell envelope which could contribute to ligand classes W and X include LPS, although phosphate levels in the LPS of cyanobacteria are reported to be generally low (7, 18, 36, 47). Lipids present in the cell wall may also exhibit phosphoryl groups, such as phosphatidylglycerol and phosphatidylcholine, which are found in the cell wall of the cyanobacterium *Synechocystis* sp. strain PCC 6714 (21). Interestingly, the cell wall polymers of cyanobacteria exhibit lower phosphate levels than those of other gram-negative bacteria. In consideration of this, it is speculated that ligand class W may be associated with the band of carboxyl groups represented by ligand classes U and V.

Ligand class Y is the least abundant class and could be associated with either the phosphoryl-ligand class X cluster or the amine-ligand class Z cluster. Finally, ligand class Z, which exhibits a mean pK_a of 8.92, is likely representative of amine functional groups. These occur in abundance within the peptidoglycan (peptide part), in proteins embedded in the outer membrane, and also within the sheath (as described above). The division of pK_a groups into ligand classes is somewhat arbitrary (5), and it would be possible to further divide classes X and Z into two groups each. However, this would have a negligible effect on the conclusions, as both peaks would still be attributed to phosphoryl and amine groups, respectively.

It is clear that the cyanobacterial surface is composed of an intricate array of complex biological molecules (7, 18, 20, 21, 23, 36, 46, 47), resulting in a high degree of chemical heterogeneity in the cell envelope. As a result, electronic and steric interactions within this complex arrangement can be quite large (5, 43), and thus the pK_a of a functional group will be influenced by the group's location within this highly reactive meshwork. Thus, any given functional group type is likely to exhibit a range of pK_a that is dependent on its distribution throughout the cell envelope. This is highlighted by the array of discrete proton binding sites (ligand classes) described above. For example, the three main functional groups (carboxyl, phorphoryl, and amine) present on whole, intact filaments produced six potentially discrete binding sites (Fig. 3 and Table

2). The pK_a clusters could arguably be grouped into less than six ligand classes, but this may not reflect the true complexity and heterogeneity of proton binding sites in the cell envelope (5). Interestingly, a comparison of the pK_a spectra for sheath material (Fig. 2) and whole filaments (Fig. 3) demonstrates well the effects of structural and chemical complexity on the generated pK_a spectra. Figure 2 shows that the structurally and chemically simpler sheath produces a pK_a spectrum which falls into five more easily defined discrete ligand classes. In comparison, the intricate structure of the cell envelope as a whole produces a more complex spectrum (Fig. 3), as though representing a more continuous and complex spectrum of binding sites. The heterogeneity of reactive proton binding sites (i.e., the distribution of ligand classes and standard deviations for mean pK_a and mean site densities) found in this study does compare well with values obtained previously for other bacterial surfaces (5, 41).

Interpretation of EPM analyses. As described earlier, EPM analyses of isolated sheath fragments indicate that the sheath exhibits a net surface charge that is close to neutral at pH 5.5 (Fig. 4a). This net neutrality is consistent with a low concentration of functional groups upon the sheath and implies that the dominant, negatively charged carboxyl and positively charged amine groups, present at mid-pHs, must occur in approximately equal proportions. The slight increase in the negative charge of the sheath with increasing pH (Fig. 4a) is suggested to be predominantly a result of deprotonation of carboxylic and phosphoric groups to form negatively charged species but may also be contributed to by deprotonation of amine groups to form electroneutral species.

Of further interest are the dual peaks observed during EPM analyses of fragmented whole filaments (Fig 4b). Based upon comparative values obtained in this study for *Bacillus subtilis* (-2.24 μm/s/V/cm) and *Escherichia coli* (-3.6 μm/s/V/cm), both bacteria that lack extracellular capsules or sheaths (data not shown), it is suggested that the most electronegative peak, around -2.5 μm/s/V/cm, is representative of cells that have been unsheathed and of some cell wall fragments, both produced during filament breakage in the tissue grinder. The broader peak at 0 to -1 μm/s/V/cm is probably representative of ensheathed filaments or of separated sheath material. As EPM is an indication of surface charge, one would expect the ensheathed filament peak in Fig. 4b to be identical to the isolated sheath peak in Fig. 4a. Although the peaks are very similar, the slight negative shift between the peak for the isolated sheath material (average, $+0.1$ μm/s/V/cm) and that for the ensheathed filaments (average, -0.5 μm/s/V/cm) is probably a result of the exposure of negatively charged cell wall material at the fragmented ends of each ensheathed filament.

Further discussion of and implications for the surface reactivity of *Calothrix* strain KC97. Interestingly, the total ligand concentrations exhibited by both whole filaments and isolated sheath material were similar, at 80.3×10^{-5} mol/g of cyanobacteria and 82.3×10^{-5} mol/g of sheath material, respectively. However, quantitative cell fractionation established that the sheath comprises only ~15% of the total dry mass of whole filaments and thus of the 80.3×10^{-5} mol of reactive surface sites/g displayed by whole filaments, only 12.3×10^{-5} mol/g is contributed by the sheath. From this, it is evident that in *Calothrix* sp. strain KC97, much of the surface reactivity is located on the cell wall, and the sheath by comparison is relatively unreactive. The observation that much of the surface reactivity is located on the cell wall is corroborated by the near-neutral EPM of the isolated sheath material. Furthermore, EPM analysis of fragmented filaments shows that they separate into a highly electronegative fraction suggested to be unsheathed cells and a weakly electronegative fraction representative of sheathed filaments. Additional evidence for the charge distribution between the sheath and cell wall was clearly illustrated by TEM analysis, in which the highly reactive cell wall exhibited extensive heavy metal staining in comparison to the weak staining of the less reactive sheath. Other complexities, however, may not have been detected in the present study. For example, reactive groups might not have been distributed evenly over the cell surface area, as illustrated in a study of *B. subtilis* by Sonnenfeld et al. (42), who found that the polar regions of the bacterium were more electronegative than the side walls. Such variation would not have been detected by the procedures used in the present study.

Interestingly, the total dry mass ligand concentration for whole filaments of *Calothrix* sp. strain KC97 compares well with values obtained for other bacteria. For example, acid-base titrations of *B. subtilis* have generated values between 22.2×10^{-5} mol/g (11) and 40×10^{-5} to 50×10^{-5} mol/g (5). Slightly higher values of 177×10^{-5} mol/g for the gram-negative species *Shewanella putrefaciens* (41) and 93×10^{-5} mol/g for isolated cell walls of *Rhodococcus erythropolis* (32) have been obtained. In these studies the proton binding sites were concentrated in one layer (i.e., the cell wall). However, for the cyanobacterium *Calothrix* sp. strain KC97, it is evident that a dual-layered system occurs (i.e., a cell wall rich in proton binding sites surrounded by a much less reactive sheath).

Whatever their exact distribution, the cyanobacterial envelope clearly contains an abundance of proton binding sites, which when deprotonated exhibit a net negative charge, and thus displays a high reactivity with cationic species in the surrounding liquid. Many studies have demonstrated how deprotonated surface functional groups rapidly bind cationic species, in particular toxic heavy metals such as Cd^{2+}, Pb^{2+}, Cu^{2+}, and UO_2^{2+} (6, 11, 13, 14, 26). These studies are performed largely to quantify how bacteria may aid in the remediation of toxic metals in contaminated water systems. The abundance of proton binding sites recorded in the cell envelope of *Calothrix* sp. strain KC97 in the present study clearly indicates the bacterium's potential for sorption of metals in natural and contaminated aquatic environments. However, it is important to consider here the effects that the dual-layered distribution of reactive sites may have on the ability of this microorganism to sequester toxic heavy metals. Although the sheath will provide some capacity to adsorb cationic metal species, much of the ability to sequester such cations will be provided by the cell wall, in which case the cationic species must be able to migrate through the sheath. The sheath's permeability is sufficient to allow a flow of nutrients and waste across the cell envelope. Thus, for ions such as H^+ (which in this study interacted with the cell wall and sheath during acid-base titration) and the metal cations mentioned above, this would not be problematic. However, the sheath of *Calothrix* sp. strain KC97 exhibits a permeability of less than 11 nm (31), and thus it is possible that some larger toxic complexes may be too great in size to migrate

through the sheath to bind to the cell wall. Further investigations are required to reveal how the dual-layered distribution of reactive sites of *Calothrix* and similar species will affect their ability to remediate toxic pollutants.

The dual-layered distribution of reactive sites may also have advantageous implications for several important ecophysiological factors. In a recent study by Phoenix et al. (31), the cyanobacterial sheath was proposed to provide a protective mechanism against detrimental biomineralization. In the case of silicification in hot springs, this exopolymer was demonstrated to act as a filter against colloidal silica by restricting silica precipitation to the sheath's outer surface and thus preventing detrimental silicification of the cell wall. In the present study, we further this premise by suggesting that the low electronegativity of the sheath may also aid in inhibiting detrimental levels of silicification. Rates of silica precipitation are increased by the presence of specific positively charged ions that act as a cation bridge between the negatively charged surfaces of the bacteria and silica colloid. In particular, Fe has been shown to dramatically increase bacterial Si precipitation (10, 28, 31; N. Yee, V. R. Phoenix, K. O. Konhauser, L. G. Benning, and F. G. Ferris, submitted for publication), with increased levels of bacterial Fe sorption correlating directly to increased levels of Si precipitation (10; Yee et al., submitted). Based on these findings, it is suggested that the relatively unreactive sheaths of microorganisms such as *Calothrix* spp. would display only a minimal ability to sequester Fe and thus rapid and detrimental silicification via cation bridging may be inhibited.

One could speculate that the low reactivity of the sheath with charged ions is also of significance for photosynthesis. During photosynthesis, cyanobacteria predominantly utilize the dissolved CO_2 species HCO_3^- as a carbon source (29). During rapid growth, there is high physiological demand for HCO_3^-, which must approach the cell via diffusion. If the sheath displayed a strong net negative charge, it would tend to retard inward diffusion of HCO_3^- by electrostatic repulsion. However, an electroneutral sheath, like that displayed by *Calothrix* sp. strain KC97, would be more inert and less resistive to inward diffusion of the HCO_3^- ion and would thus not inhibit photosynthetic uptake of this bicarbonate.

The cyanobacterium *Calothrix* sp. strain KC97 is a benthic microorganism that inhabits biofilms covering the silica sinter of the Krisuvik hot spring, Iceland. The ability of this microorganism to adhere to a substrate is fundamental to its survival in this environment, as pelagic forms would be rapidly removed from the hot spring site by the relatively fast-flowing discharge waters. A wide variety of factors may influence bacterial surface adhesion (e.g., 2, 4, 12, 39, 44). However, many studies have suggested that bacterial adhesion is proportional to the microorganism's hydrophobicity and inversely proportional to the bacterium's surface charge. For example, studies performed upon spores of *Bacillus cereus* demonstrated that spores of a hydrophobic nature are most conducive to surface attachment (19). Furthermore, adhesion increases as surface charge decreases and reaches a maximum when the surface of the spore is neutrally charged (35). Similar observations suggesting that surface charge is inversely proportional to both hydrophobicity and bacterial adhesion have been noted by Van Loosdrecht et al. (44). A study of a variety of cyanobacteria by Fattom and Shilo (9) demonstrated that benthic cyanobacteria all exhibit hydrophobic characteristics, while pelagic varieties are all hydrophilic in nature. It is possible that the hydrophobicity of benthic forms is related to their enshrouding in sheath material which displays only weak electronegativity and is therefore less likely to interact with polarized water molecules. Certainly, several species of particular interest in the study by Fattom and Shilo (9) (e.g., *Calothrix* and *Phormidium*) are known to exhibit sheath material dominated by neutral sugars and are thus weakly electronegative (17, 46). The suggestion that an enclosing sheath of low electronegativity is important in inducing hydrophobicity (and thus encouraging surface adhesion) is corroborated by observations that the free-swimming hormogonia produced by benthic cyanobacteria are all hydrophilic in nature (9). Filaments in this pelagic, transient phase lack extracellular sheaths, thus exposing the highly electronegative cell walls, which in turn may contribute significantly to the hormogonia's hydrophilic characteristic. Other studies have shown that factors which reduce the cell's effective negative surface charge (such as increased electrolyte concentration or decreases in pH) help to decrease the repulsive forces between the microorganism and the substrate and thus result in increased adhesion (16, 24). It follows that enshrouding a highly electronegative cell wall in a weakly electronegative sheath may dramatically increase the ability of *Calothrix* sp. strain KC97 to adhere to the silica sinter in the hot spring system, thus enhancing its chances of survival in such a hostile environment.

In this study we have shown that the cyanobacterium *Calothrix* sp. strain KC97 exhibits surface reactivity in terms of pK_a and proton binding site densities that is similar to that of other bacteria. The surface proton binding sites of *Calothrix* sp. strain KC97 are distributed spatially into a dual-layer system composed of a cell wall containing abundant reactive sites and a sheath that has few reactive groups. The enshroudment of the microorganism in a poorly reactive sheath layer may have important ecophysiological implications. For example, the poorly reactive sheath may inhibit detrimental biomineralization or aid diffusion of the HCO_3^- ion toward the cell during photosynthesis. Additionally, it is speculated that the low electronegativity of the sheath at most natural pH values increases the cellular hydrophobicity and thus may enhance adhesion to a substrate.

ACKNOWLEDGMENTS

We thank David Fowle for his help on the initial EPM analysis. We also thank two anonymous reviewers for their helpful comments.

This work was supported by the Natural Science and Engineering Research Council (NSERC) of Canada and through an Ontario Premier's Research Excellence Award.

REFERENCES

1. **Beveridge, T. J., and R. G. E. Murray.** 1980. Sites of metal deposition in the cell wall of *Bacillus subtilis*. J. Bacteriol. **141:**876–887.
2. **Boulange-Petermann, L.** 1996. Processes of bioadhesion on stainless steel surfaces and cleanability: a review with special reference to the food industry. Biofouling **10:**275–300.
3. **Brassard, P., J. R. Kramer, and P. V. Collins.** 1990. Binding site analysis using linear programming. Environ. Sci. Technol. **24:**195–200.
4. **Busscher, H. J., J. Sjollema, and H. C. van der Mei.** 1990. Relative importance of surface free energy as a measure of hydrophobicity in bacterial adhesion to solid surfaces, p. 335–359. *In* R. J. Doyle and M. Rosenberg (ed.), Microbial cell surface hydrophobicity. American Society for Microbiology, Washington, D.C.

5. **Cox, J. S., D. S. Smith, L. A. Warren, and F. G. Ferris.** 1999. Characterizing heterogeneous bacterial surface functional groups using discrete affinity spectrum for proton binding. Environ. Sci. Technol. **33:**4514–4521.
6. **Daughney, C. J., J. B. Fein, and N. Yee.** 1998. A comparison of the thermodynamics of metal adsorption onto two common bacteria. Chem. Geol. **144:**161–176.
7. **Drews, G., and J. Weckesser.** 1982. Function, structure and composition of cell walls and external layers, p. 333–357. *In* N. G. Carr and B. A. Whitton (ed.), The biology of cyanobacteria. Blackwell Scientific Publications, Oxford, England.
8. **Dudman, W. F.** 1977. The role of surface polysaccharides in natural environments, p. 357–414. *In* I. Sutherland (ed.), Surface carbohydrates of the prokaryotic cell. Academic Press Inc., London, England.
9. **Fattom, A., and M. Shilo.** 1984. Hydrophobicity as an adhesion mechanism of benthic cyanobacteria. Appl. Environ. Microbiol. **47:**135–143.
10. **Fein, J. B., S. Scott, and N. Rivera.** 2002. The effect of Fe on Si adsorption by Bacillus subtilis cell walls: insights into non-metabolic bacterial precipitation of silicate minerals. Chem. Geol. **182:**265–273.
11. **Fein, J. B., C. J. Daughney, N. Yee, and T. A. Davis.** 1997. A chemical equilibrium model for metal adsorption onto bacterial surfaces. Geochim. Cosmochim. Acta **61:**3319–3328.
12. **Fletcher, M.** 1996. Bacterial attachment in aquatic environments: a diversity of surfaces and adhesion strategies, p. 1–24. *In* M. Fletcher (ed.), Bacterial adhesion: molecular and ecological diversity. John Wiley & Sons, New York, N.Y.
13. **Fowle, D. A., and J. B. Fein.** 2001. Quantifying the effects of *Bacillus subtilis* cell walls on the precipitation of copper hydroxide from aqueous solution. Geomicrobiol. J. **18:**77–91.
14. **Fowle, D. A., J. B. Fein, and A. M. Martin.** 2000. Experimental study of uranyl adsorption onto *Bacillus subtilis.* Environ. Sci. Technol. **34:**3737–3741.
15. **Gimmler, H., J. de Jesus, and A. Greiser.** 2001. Heavy metal resistance of the extreme acidotolerant filamentous fungus *Bispora* sp. Microb. Ecol. **42:**87–98.
16. **Gingell, D., and S. Vince.** 1980. Long-range forces and adhesion: an analysis of cell-substratum studies, p. 1–37. *In* A. S. C. Curtis and J. D. Pitts (ed.), Cell adhesion and motility. Cambridge University Press, Cambridge, England.
17. **Hoiczyk, E.** 1998. Structural and biochemical analysis of the sheath of *Phormidium uncinatum*. J. Bacteriol. **180:**3923–3932.
18. **Hoiczyk, E., and A. Hansel.** 2000. Cyanobacterial cell walls: news from an unusual prokaryotic envelope. J. Bacteriol. **182:**1191–1199.
19. **Husmark, U., and U. Ronner.** 1990. Forces involved in the adhesion of *Bacillus cereus* spores to solid surfaces under different environmental conditions. J. Appl. Bacteriol. **69:**557–562.
20. **Jürgens, U. J., G. Drews, and J. Weckesser.** 1983. Primary structure of the peptidoglycan from the unicellular cyanobacterium *Synechocystis* sp. strain PCC 6714. J. Bacteriol. **154:**471–478.
21. **Jurgens, U. J., J. R. Golecki, and J. Weckesser.** 1985. Characterization of the cell wall of the unicellular cyanobacterium *Synechocystis* PCC 6714. Arch. Microbiol. **142:**168–174.
22. **Jurgens, U. J., and W. Mantele.** 1991. Orientation of carotenoids in the outer membrane of *Synechocystis* PCC 6714 (cyanobacteria). Biochim. Biophys. Acta **1067:**208–212.
23. **Jürgens, U. J., and J. Weckesser.** 1986. Polysaccharide covalently linked to the peptidoglycan of the cyanobacterium *Synechocystis* sp. strain PCC6714. J. Bacteriol. **168:**568–573.
24. **Marshall, K. C., R. Stout, and R. Mitchell.** 1971. Mechanisms of the initial events in the sorption of marine bacteria to surface. J. Gen. Microbiol. **68:**337–348.
25. **Martell, A. E., and R. M. Smith.** 1987. Critically selected stability constants of metal complexes database version 4.0. Texas A&M University, College Station.
26. **Martinez, R. E., and F. G. Ferris.** 2001. Chemical equilibrium modeling techniques for the analysis of high-resolution bacterial metal sorption data. J. Colloid Interface Sci. **243:**73–80.
27. **Matz, C., and K. Jürgens.** 2001. Effects of hydrophobic and electrostatic cell surface properties of bacteria on feeding rates of heterotrophic nanoflagellates. Appl. Environ. Microbiol. **67:**814–820.
28. **Mera, M. U., and T. J. Beveridge.** 1993. Mechanisms of silicate binding to the bacterial cell wall in *Bacillus subtilis*. J. Bacteriol. **175:**1936–1945.
29. **Miller, A. G., and B. Colman.** 1980. Evidence for HCO_3^- transport by the blue-green alga (cyanobacterium) Coccochloris peiocyctis. Plant Physiol. **65:**397–402.
30. **Perdue, E. M.** 1985. Acidic functional groups of humic substances, p. 493–526. *In* G. R. Aiken, D. M. McKnight, R. L. Wershaw, and P. MacCarthy (ed.), Humic substances in soil, sediment and water. John Wiley & Sons, New York, N.Y.
31. **Phoenix, V. R., D. G. Adams, and K. O. Konhauser.** 2000. Cyanobacterial viability during hydrothermal biomineralization. Chem. Geol. **169:**329–338.
32. **Plette, A. C. C., W. H. Vanriemsdijk, M. F. Benedetti, and A. Vanderwal.** 1995. pH dependent charging behaviour of isolated cell-walls of a gram-positive soil bacterium. J. Colloid Interface Sci. **173:**354–363.
33. **Resch, C. M., and J. Gibson.** 1983. Isolation of the carotenoid-containing cell wall of three unicellular cyanobacteria. J. Bacteriol. **155:**345–350.
34. **Rippka, R., J. Deruelles, J. B. Waterbury, M. Herdman, and R. Y. Stainer.** 1979. Generic assignments, strain histories and properties of pure cultures of cyanobacteria. J. Gen. Microbiol. **111:**1–61.
35. **Ronner, U., U. Husmark, and A. Henriksson.** 1990. Adhesion of bacillus spores in relation to hydrophobicity. J. Appl. Bacteriol. **69:**550–556.
36. **Schmidt, W., G. Drews, J. Weckesser, and H. Mayer.** 1980. Lipopolysaccharides in four strains of the unicellular cyanobacterium *Synechocystis*. Arch. Microbiol. **127:**217–222.
37. **Schrader, M., G. Drews, and J. Weckesser.** 1981. Chemical analysis on cell wall constituents of the thermophilic cyanobacterium *Synechococcus* PCC 6716. FEMS Microbiol. Lett. **11:**37–40.
38. **Scott, C., R. L. Fletcher, and G. B. Bremer.** 1996. Observations of the mechanisms of attachment of some marine fouling blue-green algae. Biofouling **10:**161–173.
39. **Sharma, P. K., K. Hanumantha Rao, K. S. E. Forssberg, and K. A. Natarajan.** 2001. Surface chemical characterization of Paenibacillus polymyxa before and after adaptation to sulfide minerals. Int. J. Miner. Processing **62:**3–25.
40. **Smith, S. D., N. W. H. Adams, and J. R. Kramer.** 1999. Resolving uncertainty in chemical speciation determinations. Geochim. Cosmochim. Acta **63:**3337–3347.
41. **Sokolov, I., D. S. Smith, G. S. Henderson, Y. A. Gorby, and F. G. Ferris.** 2001. Cell surface electrochemical heterogeneity of the Fe(III)-reducing bacteria *Shewanella putrefaciens*. Environ. Sci. Technol. **35:**341–347.
42. **Sonnenfeld, E. M., T. J. Beveridge, and R. J. Doyle.** 1985. Discontinuity of charge on the cell wall poles of *Bacillus subtilis.* Can. J. Microbiol. **31:**875–877.
43. **Stone, A. T.** 1997. Reactions of extracellular organic ligands with dissolved metal ions and mineral surfaces, p. 309–344. *In* J. F. Banfield and K. H. Nealson (ed.), Geomicrobiology: interactions between microbes and minerals. Mineralogical Society of America, Washington, D.C.
44. **Van Loosdrecht, M. C. M., J. Lyklema, W. Norde, G. Schraa, and A. J. B. Zehnder.** 1987. The role of bacterial cell wall hydrophobicity in adhesion. Appl. Environ. Microbiol. **53:**1893–1897.
45. **Van Loosdrecht, M. C. M., J. Lyklema, W. Norde, G. Schraa, and A. J. B. Zehnder.** 1987. Electrophoretic mobility and hydrophobicity as a measure to predict the initial steps of bacterial adhesion. Appl. Environ. Microbiol. **53:**1898–1901.
46. **Weckesser, J., K. Hofmann, U. J. Jurgens, B. A. Whitton, and B. Raffelsberger.** 1988. Isolation and chemical analysis of the sheaths of the filamentous cyanobacteria *Calothrix parienta* and *C. scopulorum*. J. Gen. Microbiol. **134:**629–634.
47. **Weckesser, J., A. Katz, G. Drews, H. Mayer, and I. Fromme.** 1974. Lipopolysaccharide containing L-acofriose in the filamentous blue-green alga *Anabaena variabilis*. J. Bacteriol. **120:**672–678.
48. **Wilson, W. W., M. M. Wade, S. C. Holman, and F. R. Champlin.** 2001. Status of methods for assessing bacterial cell surface charge properties based on zeta potential measurements. J. Microbiol. Methods **43:**153–164.